AGU PUBLICATIONS

JGR

Journal of Geophysical Research: Atmospheres

RESEARCH ARTICLE

10.1002/2017JD027206

Key Points:

- Time correlation of lightning flashes is studied based on analysis of lightning VHF data of 40 thunderstorms with DFA, AF, and FF methods
- It is found that lightning flashes behaves long timely correlated but short timely random, with an average crossover time of 114 s
- The results imply that the occurring time of lightning flashes is highly related to the common thunderstorm electrification process

Correspondence to:
M. Chen,
mingli.chen@polyu.edu.hk

Citation:
Gou, X., Chen, M., & Zhang, G. (2018). Time correlations of lightning flash sequences in thunderstorms revealed by fractal analysis. *Journal of Geophysical Research: Atmospheres*, *123*, 1351–1362. https://doi.org/10.1002/2017JD027206

Received 26 MAY 2017
Accepted 8 JAN 2018
Accepted article online 13 JAN 2018
Published online 29 JAN 2018

Time Correlations of Lightning Flash Sequences in Thunderstorms Revealed by Fractal Analysis

Xueqiang Gou[1], Mingli Chen[2], and Guangshu Zhang[3]

[1]College of Physics and Electronic Engineering, Northwest Normal University, Lanzhou, China, [2]Department of Building Services Engineering, The Hong Kong Polytechnic University, Hong Kong, [3]Cold and Arid Regions Environmental and Engineering Research Institute, Chinese Academy of Sciences, Lanzhou, China

Abstract By using the data of lightning detection and ranging system at the Kennedy Space Center, the temporal fractal and correlation of interevent time series of lightning flash sequences in thunderstorms have been investigated with Allan factor (AF), Fano factor (FF), and detrended fluctuation analysis (DFA) methods. AF, FF, and DFA methods are powerful tools to detect the time-scaling structures and correlations in point processes. Totally 40 thunderstorms with distinguishing features of a single-cell storm and apparent increase and decrease in the total flash rate were selected for the analysis. It is found that the time-scaling exponents for AF (α_{AF}) and FF (α_{FF}) analyses are 1.62 and 0.95 in average, respectively, indicating a strong time correlation of the lightning flash sequences. DFA analysis shows that there is a crossover phenomenon—a crossover timescale (τ_c) ranging from 54 to 195 s with an average of 114 s. The occurrence of a lightning flash in a thunderstorm behaves randomly at timescales $<\tau_c$ but shows strong time correlation at scales $>\tau_c$. Physically, these may imply that the establishment of an extensive strong electric field necessary for the occurrence of a lightning flash needs a timescale $>\tau_c$, which behaves strongly time correlated. But the initiation of a lightning flash within a well-established extensive strong electric field may involve the heterogeneities of the electric field at a timescale $<\tau_c$, which behave randomly.

1. Introduction

Lightning discharge is a fundamentally multiscale (fractal) event, spanning from less than a meter to many kilometers in space. It radiates electromagnetic waves across a broad frequency band, ranging from below 1 Hz to near 300 MHz, and even high frequencies like microwave and optical wave (Rakov & Uman, 2003). Using the time of arrival locating method in the VHF (very high frequency) regime, such as lightning mapping array (Krehbiel et al., 2000; Rison et al., 1999; Thomas et al., 2004) and LDAR (lightning detection and ranging) (Maier et al., 1995), a large amount of high-resolution data of VHF radiation sources in lightning event are obtained. And with these VHF data, more details of lightning processes are revealed and apparent fractal behaviors are evidenced (Bruning & Thomas, 2015).

There are many researches on the fractal behavior of the development of a lightning flash in thunderstorm. Based on the well-known bidirectional leader concept of lightning initiation and propagation (Mazur, 2002), many numerical models are advanced in terms of modeling of spatial morphological features, particularly the spectacular fractal feature, of lightning events (Mansell et al., 2002; Riousset et al., 2007; Hayakawa et al., 2008; Iudin & Davydenko, 2015). However, there is a problem that some important features, such as the intermittency and polarity asymmetry in lightning initiation and propagation (Gou et al., 2010; Van der Velde & Montanya, 2013; Williams, 2006; Williams & Heckman, 2012), which are closely related, are too elusive to be consistently included in the model work (Da Silva, 2015). As a matter of fact, the bursts of lightning VHF radiation events observed are dominant with negative polarity (Thomas et al., 2001). There are two types of negative breakdown: the initial breakdown due to leader extension in virgin air and the recoil breakdown due to instability of channel characteristic of either the negative differential resistance (Williams & Heckman, 2012) or the screening effect of branched channel (Mazur, 2002; Mazur, 2016). Both breakdowns are found to show collective behaviors (cluster and synchronicity) in VHF radiation events (Gou et al., 2010; Huang et al., 1997). The collective behavior of lightning flash sequence in thunderstorm is further evidenced in works of Telesca et al. (2005), Hayakawa et al. (2005, 2008); Yair et al. (2006); Yair et al. (2009), and Zoghzoghy et al. (2013).

The strong burst and collective behavior of lightning VHF events, which often makes the analysis difficult, however, are well consistent with the theory of general fractal and evolutionary dynamics of catastrophic event in nature. According to this theory, a large-scale breakdown event is more controlled by the cooperativity and scaling up of small-scale breakdown interactions. A small-scale breakdown event may only occur in the random phase. As the breakdown increases, a new "phase" appears and small-scale breakdown events begin to interact and merge, leading to screening and other cooperative effects. A large-scale breakdown event is possible only on electrical field regions correlated to sufficient lengths, characterized by the stochastic (avalanche) and regular (scale-free) fractal behaviors in VHF radiations (Bak et al., 1987; Turcotte et al., 2002; Sornette, 2004).

By scaling analyses, such as detrended fluctuation analysis (DFA) (Peng et al., 1994), Allan factor (AF) analysis, Fano factor (FF) analysis (Telesca, 2007; Telesca et al., 2005), and discrete scale invariance (DSI) analysis (Saleur et al., 1996; Sornette, 2004), some important revolutionary processes of a fractal system, such as the long-range correlation associated with the global instability, can be well revealed.

To further our understanding of the fractal behavior and possible correlation between lightning flashes in a thunderstorm, which may be an important factor to understand the rule of establishment (electrification) of strong electric field necessary for a lightning flash to occur, we aim to have a systematic investigation of the interdependence of lightning flashes based on large amount of LDAR data. In the present study, by applying the DFA, AF, and FF analyses to three-dimensional VHF source data from LDAR, the temporal fractal and correlation behavior of lightning flash sequences in thunderstorms is investigated. Meanwhile, the physical implications of the lightning initiation behind the fractal analysis results are discussed.

2. Method

A lightning flash is developed from hundreds to thousands of small-scale breakdown processes, which is proven to have fractal cluster property. But how about the relations between lightning flashes occurring in the same thunderstorm? Are they correlated or nonrelated to each other? To answer this question, we consider the lightning flash sequence in a thunderstorm, like any other natural hazards, such as earthquakes, rain, and volcanic eruptions, as a stochastic point process characterized by the lightning flash occurrence times. Such a process may be called a fractal system if some relevant statistics show scaling (power law) with related scaling exponents.

The standard method to investigate the presence of fractal and correlation in a time series is to get the power spectral density $S(f)$ by means of a Fourier transform of the time series. If the $S(f)$ of a time series decreases as a power law function of the frequency f as $S(f) \sim f^{-\alpha}$ (where $\alpha > 0$ is the scaling exponent which quantifies the strength of time correlations) and α is larger than certain value, then the time series is called a fractal and time-correlated process. For a point process, like lightning flash sequence, simple application of the Fourier transform is not possible. Thus, other scaling methods such as FF and AF analyses are designed to extract the correlation exponent.

A point process is usually described by a set of event occurrence times $\{t_i\}$. Other two equivalent ways used to describe it are as follows: (i) the interevent interval series $\tau(i) = t_{i+1} - t_i$ and (ii) the counting process $N_k(\tau)$ that is produced by dividing the whole time interval into equally spaced contiguous counting windows of the duration τ and counting the number of events $N_k(\tau)$ in the kth window. Both approaches assume that the indexes of the events serve as a kind of internal "clock" marking the time (Abe & Suzuki, 2012; Varotsos et al., 2011). In this study we use three statistical measures: DFA, AF, and FF. The former one is related to the interevent interval representation, while the remaining two are related to the counting process representation.

2.1. Detrended Fluctuation Analysis

Detrended fluctuation analysis (DFA) is a well-known methodology which permits the detection of long-range correlation in observational time series possibly affected by nonstationarities. The DFA procedure consists of four steps.

Step 1: For a given time series $x(i)$, $i = 1, \ldots, N$, determine the "profile" relative to its mean $< x >$,

$$Y(k) = \sum_{i=1}^{k} (x(i) - < x >). \tag{1}$$

Step 2: Divide $Y(i)$ into M_s = int (N/s) nonoverlapping segments of the length s starting from both the beginning and the end of the time series (i.e., $2M_s$ such segments in total). For each of segment v and scale s, calculate the root-mean-square fluctuation function $F(v, s)$,

$$F(v,s) = \sqrt{\frac{1}{s}\sum_{k=1}^{s}\left(Y_v(k) - Y_{n,v}(k)\right)^2}, \tag{2}$$

where $Y_{v,\,n}$ is the nth order polynomial fitting of the vth segment Y_v.

Step 3: Calculate the fluctuation function,

$$F(s) = \sqrt{\frac{1}{2M_s}\sum_{v=1}^{2M_s}|F(v,s)|^2}. \tag{3}$$

Step 4: Determine the scaling behavior of the fluctuation by analyzing the log-log plot of $F_q(s)$ versus s,

$$F(s) \sim s^{\alpha}, \tag{4}$$

where α is the Hurst index quantifying the strength of long-range power law correlations of the time series events $x(i)$. If $\alpha = 0.5$, the temporal fluctuations (the events) are uncorrelated. If $\alpha > 0.5$, correlations among the events are persistent, meaning that a large (small) value (compared to the average) is more likely to be followed by a large (small) value, of which the underlying dynamics is governed by positive feedback mechanisms. If $\alpha < 0.5$, correlations among the events are antipersistent, meaning that a large (small) value (compared to the average) is more likely to be followed by a small (large) value, of which the underlying dynamics is governed by negative feedback mechanisms. If $\alpha = 1$, it indicates a flicker noise dynamics, meaning a typical system in a self-organized critical state.

2.2. Fano Factor

Fano factor (FF), which is a measure of the dispersion of a temporal point process, is defined as the ratio of the variance to the mean,

$$FF(\tau) = \frac{< N_k^2(\tau) > - < N_k(\tau)>^2}{< N_k(\tau) >}. \tag{5}$$

If the point process is time correlated, FF(τ) shall grow in a power law form

$$\mathrm{FF}(\tau) = 1 + \left(\frac{\tau}{\tau_0}\right)^{\alpha}, \tag{6}$$

where α ($0 < \alpha < 1$) is the scaling exponent and τ_0 is the fractal onset time marking the lower limit for a significant scaling behavior. $\alpha \approx 0$ features a Poisson point process FF(τ) = 1, and $\alpha > 0.5$ features an obvious fractal and correlative process.

2.3. Allan Factor

Allan factor (AF), which is related to the variability of successive counts, is defined as the ratio of Allan variance to twice the mean

$$\mathrm{AF}(\tau) = \frac{\left\langle (N_{k+1}(\tau) - N_k(\tau))^2 \right\rangle}{2\langle N_k(\tau)\rangle}, \tag{7}$$

which is related to FF(τ) by

$$\mathrm{AF}(\tau) = 2\mathrm{FF}(\tau) - \mathrm{FF}(2\tau). \tag{8}$$

Like FF(τ), for a time-correlated point process, AF(τ) varies in a power law form

$$\mathrm{AF}(\tau) = 1 + \left(\frac{\tau}{\tau_1}\right)^{\alpha} \tag{9}$$

where α ($0 < \alpha < 3$) is the scaling exponent and τ_1 is another fractal onset time. Both FF(τ) and AF(τ) measure the dispersion and time correlation of a point process referred to the benchmark Poisson process in which $\alpha_{FF} = \alpha_{AF} = 0$ and FF(τ) = AF(τ) = 1 for all τ. In contrast to FF(τ), AF(τ) can be used to estimate scaling exponents over the expanded range (larger than 1). The larger the α_{AF} is, the stronger the time correlation among the point process. Furthermore, the difference of successive counts is considered in AF(τ) to reduce the effect of possible nonstationary of the point process.

3. LDAR Data and Preprocessing

3.1. LDAR System

LDAR is a three-dimensional lightning VHF detection network, developed primarily by Lennon at Kennedy Space Center in mid-1970s and later improved in early 1990s (Lennon & Maier, 1991; Maier et al., 1995). It contains six outlying stations in an approximately circular array about 20 km in diameter around a seventh controlling station located at latitude 28.548 N and longitude 80.648 W.

LDAR operates at 66 MHz (VHF) with a bandwidth of 6 MHz, sensing electromagnetic emissions from lightning breakdown and channel formation processes. Three-dimesional locations of the lightning VHF sources are derived from the difference in the time of arrival of the signal detected at different receivers. The time resolution of LDAR is 10 ns, and the time window for examining individual pulses is 80 μs. The location accuracy is about 100 m in its interior and 1 km or less within 40 km. The detection efficiency of LDAR is to be 99% within 25 km of the central site (Maier et al., 1995).

3.2. Flash Grouping

LDAR data are available for download from the Global Hydrology Resource Center. In conducting the research, we first group the large numbers of individual radiation sources of LDAR data into discrete lightning flashes according to specific temporal and spatial constraints. The Interactive Data Language flash-grouping algorithm for the LDAR sensor, developed by Murphy et al. (2000) and extended by Nelson (2002) and McNamara (2002), is adopted; see also Hansen et al. (2010) and Stano et al. (2010). The algorithm first removes the calibration data and then uses temporal and spatial constraints to group data points into flashes. For a data point to be included in a flash, it must occur within 3 s of the first data point in the flash, and a successive point must have occurred within 0.5 s of the previous data point in the flash. For the spatial constraint of a data point to be included in a flash, an ellipse with major and minor axes of 5,000 m plus LDAR's radial and azimuthal errors in locating the data point is created around the data point. If the previous data point included in the flash is within the ellipse, the data point under consideration is included in the current flash. Otherwise, the data point is excluded from the current flash.

After flash grouping, data points within a flash are further grouped into branches based on another set of temporal and spatial constraints. To be part of a branch, a data point must be within 0.03 s of the previous data point in the same branch. The spatial constraint is again a function of the data point's distance from LDAR central site. Once all data points are grouped into flashes and branches, the results are written to an output file, which includes each original LDAR data point (occurring time and three-dimensional location) and an index indicating the sequential number of that data point within a branch of a flash and so on.

4. Results

We have checked all the flash data from 1997 to 2007, only those flashes originating within 90 km of LDAR central site were used in this study. The reason for doing this is that LDAR's effective usable distance for scientific study is approximately within this distance (Boccippio et al., 2001). In addition, a flash with the VHF source number less than 10 was filtered out and not included in the flash sequence for AF and FF analyses. Imposing the 10-source criterion, as demonstrated by Wiens et al. (2005), will not affect the determination of the trend in total lightning but can eliminate noise points that the LDAR might misclassify as a flash.

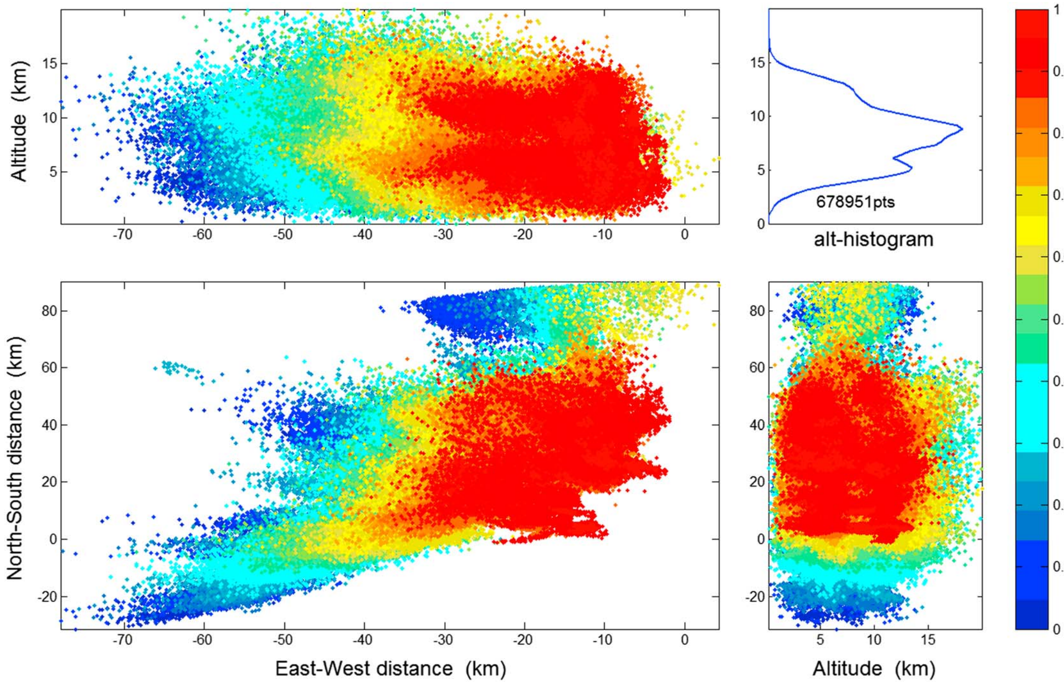

Figure 1. A multipanel plot of LDAR VHF sources (colored points) for a 93 min period beginning at 20:22:21 UTC on 7 August 2003 of a selected thunderstorm. Sources are colored by time from blue to red. (top left) *X-Z* cross-section view of the VHF sources. (top right) The VHF source frequency histogram with altitude. (bottom left) *X-Y* plan view. (bottom right) The *Y-Z* view of the VHF sources. Distances are referred to the center station of LDAR.

After flash grouping of LDAR data, the flash data set was further selected using certain temporal and spatial constraints. For temporal constraint, we looked for a relatively complete and long (more than 1 h) evolution circle featured with a large flash peak rate, including apparent increase and decrease of the flash rate. In doing this, first, all flashes were binned into each UTC minute to arrive at a flash rate, that is, the total number of flashes in each minute. Second, the plot of 1 min time flash rate versus time was smoothed using a two-point moving average method. Then, the time period of data was tentatively selected manually to examine whether the plot of flash rate versus time meets the temporal constraint. For spatial constraint, we focused on the isolated storm cell by manually identifying and selecting the clusters in a scatterplot. The two restriction

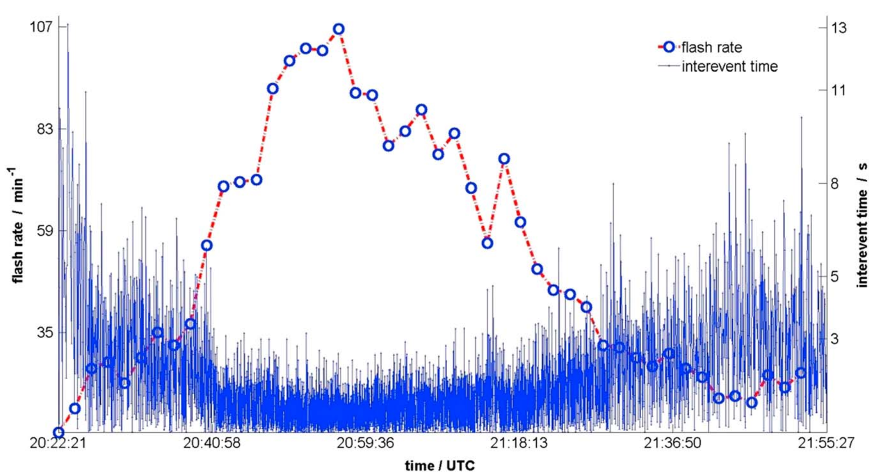

Figure 2. A plot of the 1 min total flash rate (red dotted line) and the interevent time (blue line) for flashes grouped from VHF sources of the thunderstorm shown in Figure 1.

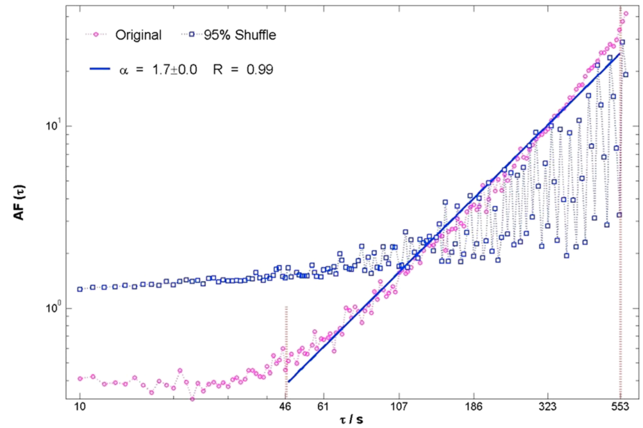

Figure 3. A log-log plot of the fluctuation AF(*s*) versus scale *s* for the interevent time intervals of lightning flashes shown in Figure 2 and that of the corresponding 95% shuffled data with identical mean and number. The thick solid line represents the linear least squares fitting of the original data. The obtained exponents and the Pearson correlation coefficients are reported in the figure. The scaleless range is indicated by the two vertical dotted lines.

procedures were repeated several times until last selection. For all the flashes examined, 40 thunderstorm cases that occurred nearby LDAR stations were selected for analyses.

Shown in Figure 1 is a multipanel plot of LDAR VHF sources (colored points) for a 93 min period beginning at 20:22:21 UTC on 7 August 2003 of a selected thunderstorm. The data contained 678,951 VHF source points, which were grouped into 4,769 flashes. No distinction is made between intracloud and cloud-to-ground flashes. Shown in Figure 2 is the 1 min total flash rate (red dotted line) and interevent time (blue line) sequence for the flashes grouped from the VHF sources of the thunderstorm shown in Figure 1.

By applying AF, FF, and DFA methods to the interevent time sequence of flashes grouped from VHF sources in each thunderstorm, factors FF and AF have been calculated for timescales τ ranging from 10 s to *T*/10 for all the 40 thunderstorm cases, where *T* is the total period of the interevent time sequence in each thunderstorm case.

Figure 3 is the result of AF analysis of the interevent time sequences shown in Figure 2. From the figure, the following salient features can be seen: (i) the arrival process is not strictly Poissonian, since the AF curve is not flat for all timescales investigated; (ii) the time-scaling regime (the linear part of the log-log AF curve) is clearly seen from the curve. The scaleless range, indicated by two vertical dotted lines in the figure, is from 46 s to 553 s. The scaling exponent, α_{AF}, as the slope of least squares fitting line of linear part of the log-log AF curve in the figure, is estimated approximately as 1.7, which implies the presence of time correlation structures in

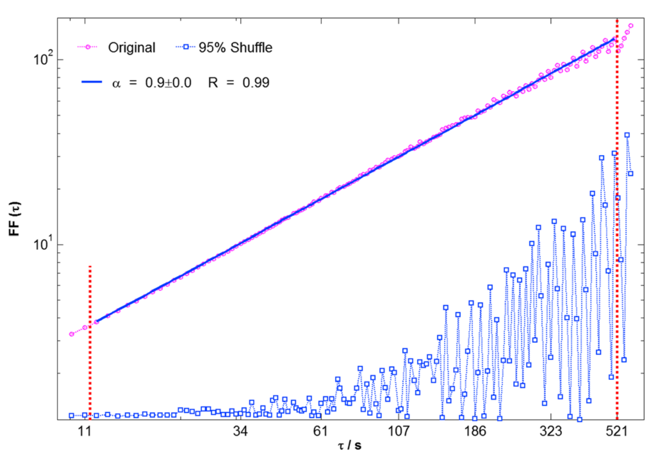

Figure 4. Same as Figure 3 but for the FF analysis.

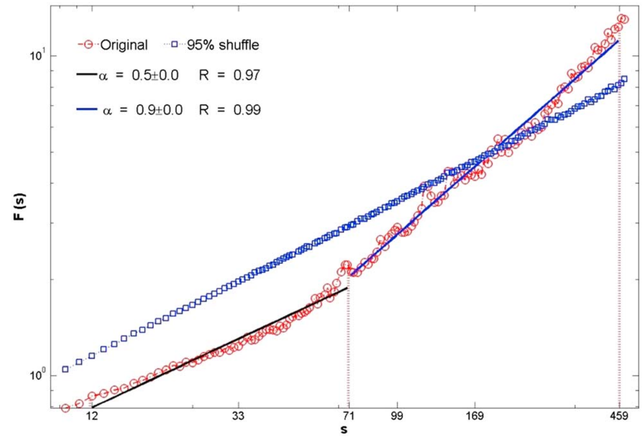

Figure 5. Same as Figure 3 but for the DFA analysis.

Table 1
A Summary of Lightning Flash Numbers Grouped From LDAR Records for the 40 Thunderstorms Analyzed

Thunderstorm/LADR packet	Flash no.
Packet_000927_235452627	4610
Packet_020801_204510305	5942
Packet_030426_203557387	4472
Packet_030603_214510035	11408
Packet_030716_165821594	4287
Packet_030722_202627053	3833
Packet_030730_222614200	4969
Packet_030801_201732172	6708
Packet_030807_201934512	4769
Packet_030812_162539729	3049
Packet_040603_194027590	3580
Packet_040604_193420699	4159
Packet_040605_192614241	9751
Packet_040611_174250001	1524
Packet_040620_211304160	4747
Packet_040627_235210427	5197
Packet_040708_174704008	9245
Packet_040712_165543126	9392
Packet_040819_181922678	7235
Packet_050804_192819135	2441
Packet_050806_191946523	3534
Packet_050812_183056322	2663
Packet_050813_174809680	6824
Packet_050815_180006401	7420
Packet_060718_170707575	4586
Packet_060724_194331399	5079
Packet_060826_173647291	2505
Packet_070607_192301082	6045
Packet_070611_183037596	1957
Packet_970804_195025401	7153
Packet_970805_172423139	4973
Packet_970811_185948724	5975
Packet_970816_173057255	4300
Packet_980706_191153090	3086
Packet_980712_185537363	2429
Packet_980806_173127302	5528
Packet_980815_172458353	8779
Packet_990821_185213100	3964
Packet_990907_150821568	3477
Packet_990907_172002381	7061

the interevent time distribution of the lightning flash sequence in the thunderstorm. The Pearson correlation coefficients (*R*), which measures the goodness of the fitting, is as high as 0.99.

In order to check whether the scaling behavior of the sequence is due to the shape of probability density function of interevent times or due to their orderings, a shuffled version of surrogate data (shuffled data) test (Theiler et al., 1992) was performed. The shuffled data were generated by randomly permuting the temporal order of the interevent time series, with the information of relative sizes of interevent time intervals remained, but all time correlations and dependencies among interevent time intervals were canceled by the shuffling procedure. For each interevent time interval sequence of lightning flashes in a thunderstorm, a set of 300 shuffled data of the original sequence was generated, and for each timescale the 95th percentile among the AF values for that timescale was calculated. The final 95% confidence of the AF curve was then given in a set of the 95th percentiles, as shown by the blue dotted square curve in Figure 3. It can be seen that the 95% confidence of the AF curve for the shuffled data is significantly different from that for the original AF curve within the scaling range. This indicates that it is the ordering of intervals that gives rise to the scaling behavior of the AF curve for the lightning flash sequence. Figure 4 is the FF result for the same sequence signal shown in Figure 2. Apart from the difference in scaling exponents, the FF result is very similar to that of the AF analysis in other aspects. The AF curve is more irregular and rougher than the FF curve, partially because that the AF is defined as the difference of counts. Meanwhile, the scaling range of the FF curve is even wider and the fitting line is almost perfect (the Pearson correlation coefficient is nearly 1).

For DFA analysis, the scale s is ranged from 4 to 1/4 of length of the series. Figure 5 is the DFA result for the same sequence signal shown in Figure 2 as well as the shuffled data. Similar to the AF and FF results, two different scaling regions are clearly detected with a crossover at scale $s_c = 71$. For the scale region lower than s_c the process is featured at random with a scaling exponent of about 0.5, while for the scale region larger than s_c the process is featured by a strong persistence with a scaling exponent of about 0.9. The timescale corresponding to the crossover scale s_c can be obtained by multiplying the crossover scale

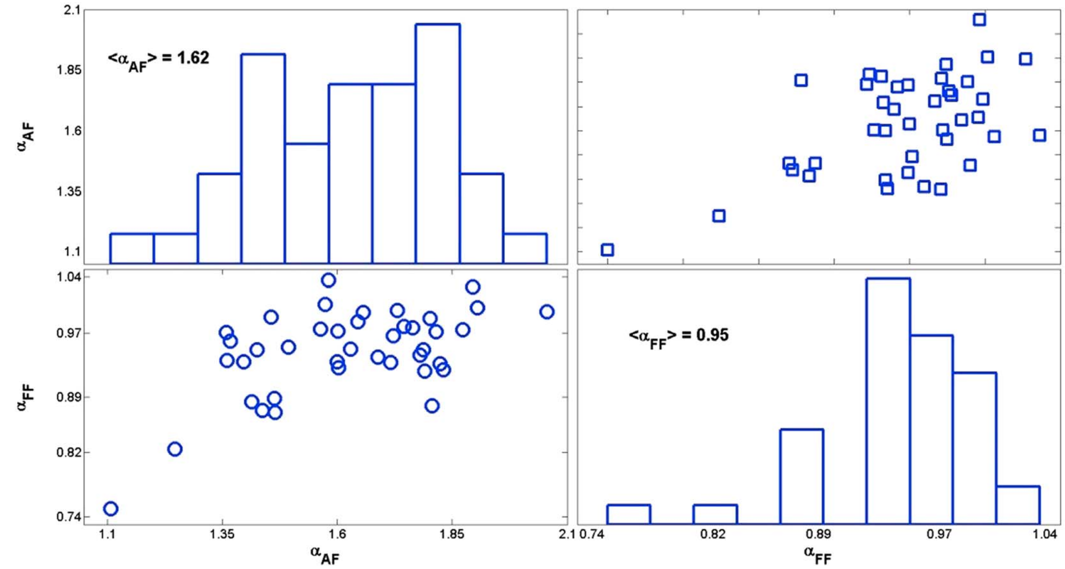

Figure 6. A matrix plot of the scaling exponents (α_{AF} and α_{AF}) for AF and FF analyses for the 40 thunderstorm cases.

s_c to the mean interevent time $< \tau > = 1.27$ s, which gives a crossover timescale $\tau_c = 88$ s. Comparing the DFA result of the original lightning flash series with that obtained on the shuffled data series, it is very obvious that the two curves are not overlapped and the scaling exponent for the shuffled data series is around 0.5, indicating a typical random process.

The results for all the 40 thunderstorm cases are very similar. The lightning flash numbers grouped from LDAR records for the 40 thunderstorms are summarized in Table 1. Shown in Figure 6 is a matrix plot of the scaling exponents (α_{AF} and α_{FF}) for AF and FF analyses for the 40 thunderstorm cases, where α_{AF} ranges from 1.11 to 2.06 with a mean of 1.62 and α_{FF} from 0.75 to 1.03 with a mean of 0.95. The Pearson correlation coefficient, R_{AF}, ranges from 0.96 to 0.99 with a mean of 0.98 and R_{FF} from 0.98 to 1.03 with a mean of 1.0.

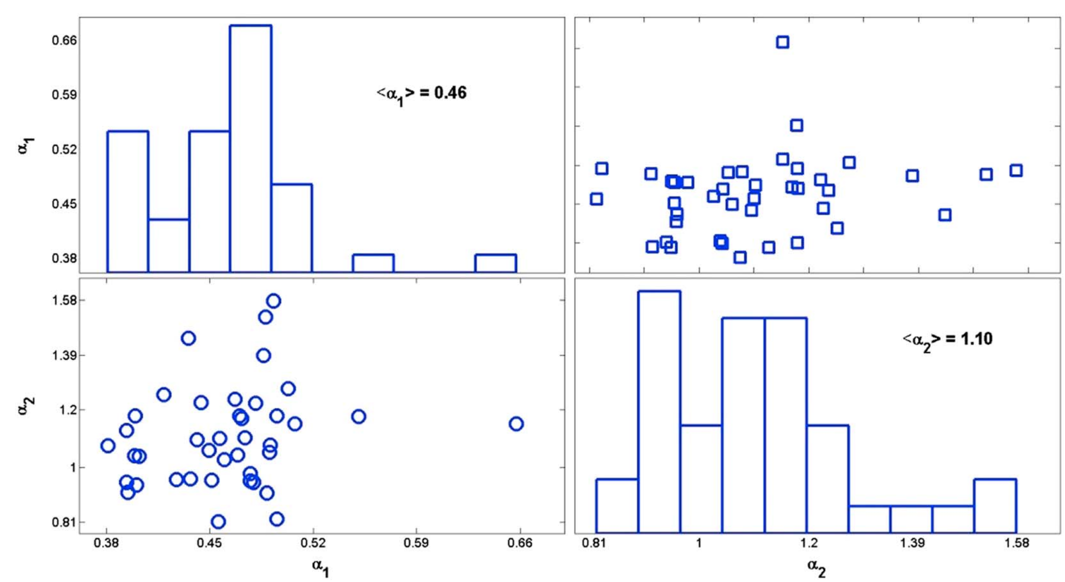

Figure 7. A matrix plot of the scaling exponents (α_1 and α_2) for DFA analysis for the 40 thunderstorm cases, where α_1 and α_2 are for the small and large scales separated by the crossover scale s_c, respectively.

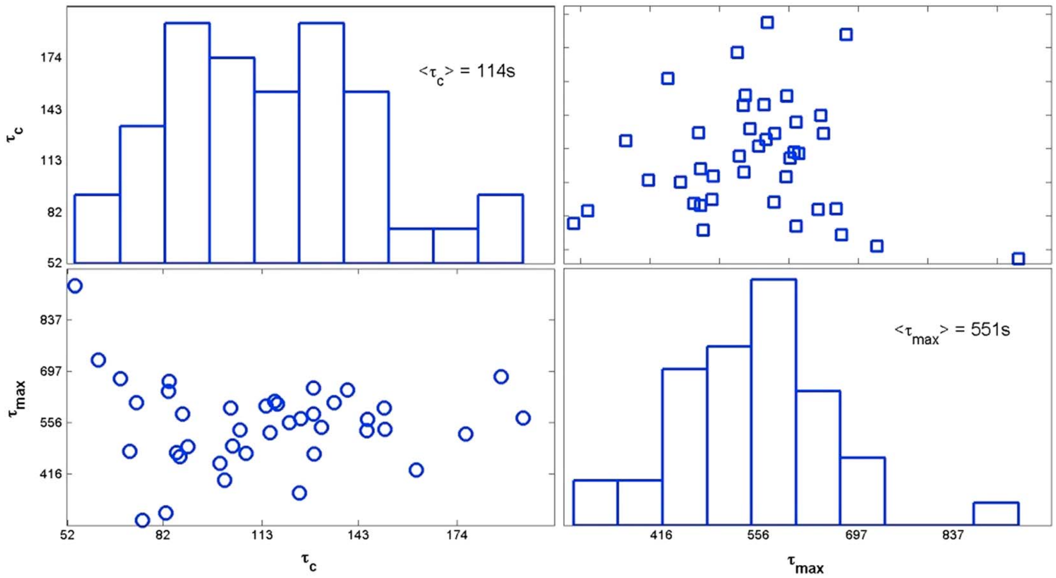

Figure 8. A matrix plot for the estimated crossover timescale τ_c and the maximum timescale τ_{max}, for DFA analysis for the 40 thunderstorms.

Figure 7 is a matrix plot of the scaling exponents (α_1 and α_2) for DFA analysis for the 40 thunderstorm cases, where α_1 and α_2 are for the small and large scales separated by the crossover scale s_c, respectively. The α_1 ranges from 0.38 to 0.66 with a mean of 0.46 and α_2 from 0.81 to 1.58 with a mean of 1.10. The Pearson correlation coefficient, R_1, ranges from 0.97 to 1.0 with a mean of 0.99 and R_2 from 0.96 to 0.99 with a mean of 0.99. Figure 8 is a matrix plot for the estimated crossover timescale τ_c and the maximum timescale τ_{max} for DFA analysis for the 40 thunderstorm cases. The τ_c ranges from 54 to 195 s with a mean of 114 s and τ_{max} from 290 to 931 s with a mean of 551 s.

To further quantify the significance of the test, for the lightning flash sequence in each thunderstorm case, the scaling exponent α_{AF} for both the original and shuffled data was calculated in the same scaling range. Let α be the scaling exponent of the original sequence, μ_s the mean, and Δ_s the standard deviation of scaling exponent of the shuffled sequence. The difference in the exponent before and after the shuffling process can be quantified as

$$\sigma = |\alpha - \mu_s|/\Delta_s, \tag{10}$$

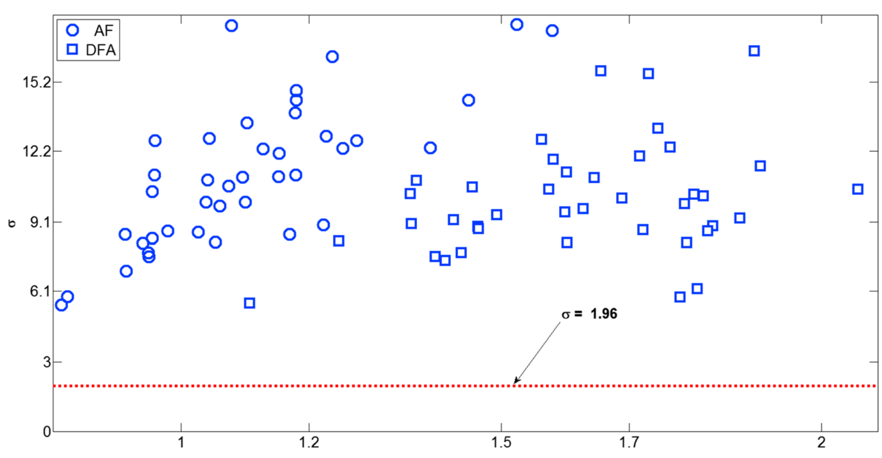

Figure 9. The scaling exponents α_{AF} and α_{DFA} versus sigma σ for the 40 thunderstorm cases analyzed. The horizontal dotted line is corresponding to $\sigma = 1.96$ ($p = 0.05$).

where σ measures the number of standard deviation of the scaling exponent of the original data apart from that of the shuffled data. The larger the σ is, the larger the separation between the exponent for the shuffled data and that for the original data. Thus, a larger σ value indicates a stronger correlation.

The significance level p is quantified as $p = \mathrm{erfc}\ (\sigma/\sqrt{2})$ (Telesca et al., 2004), which is the probability of the observing significance σ. A larger p means that the null hypothesis (absence of any correlation) is true or α values are obtained by chance.

Figure 9 shows the scaling exponents α_{AF} and α_{DFA} and their corresponding σ calculated from equation (10) for all the 40 flash sequences analyzed. The horizontal line is corresponding to $\sigma = 1.96$ ($p = 0.05$). It can be seen that all cases were time correlated and persisted with a significance level less than 0.05 ($\sigma > 1.96$).

5. Conclusions and Discussions

In this paper, we have investigated the time correlation of interevent time series of lightning flash sequences in thunderstorms with the DFA, AF, and FF analysis methods. The lightning flash sequences were obtained by grouping the VHF source data recorded by LDAR during the period of 1997 to 2007. Only those flashes originating within 90 km of LDAR central site were selected for the study. The VHF sources were first grouped into lightning flashes based on certain criteria and then the 1 min total flash rates were checked. For all the 40 thunderstorms analyzed, it is found that the scaling exponents of AF and FF analysis results (α_{AF} and α_{FF}) were about 1.62 and 0.95 in average, respectively, indicating a strong time correlation among the lightning flashes in a thunderstorm. DFA analysis further showed that there is a crossover scale (s_c) / timescale (τ_c): the lightning flash sequence in a thunderstorm showed a quite different scaling behavior over scales shorter than the crossover scale with that over scales longer than the crossover scale. For all the 40 cases, the DFA scaling exponent (α_{DFA}) for scales shorter than the crossover scale (s_c) ranged from 0.38 to 0.66 with a mean of 0.46, indicating a typical random behavior, while that for scales longer than the crossover scale (s_c) ranged from 0.81 to 1.58 with an average of 1.10, indicating a strong time-correlated behavior. The crossover timescale (τ_c) ranged from 54 to 195 s with an average of 114 s.

The above results suggest the coexistence of different dynamics related to the lightning flash sequence (occurrences) in a thunderstorm: a pure random behavior at short timescale (e.g., less than 114 s) and a strong persistence at larger timescales (e.g., larger than 114 s). Moreover, the results confirm the fact of obvious and natural correlation between all sequential lightning flashes in thunderstorms through a common process of cloud electrification in thunderstorms. This process is the time changing in its intensity, as is affected by the size of the "lightning tree" and the power of the lightning discharges. Each lightning flash, by diminishing the ambient electric field, affects the ambient electrical conditions in a larger scale, including timing of occurrence of lightning flashes which follow.

Physically, the occurrence of a lightning flash needs a strong enough electrical field established in a large enough region in a thunderstorm. The above results may imply that the establishment of an extensive strong electric field necessary for the occurrence of a lightning flash needs a timescale not less than the crossover timescale at least (e.g., about 2 min in average) and behaves strongly time correlated. However, the initiation of the lightning flash within a well-established extensive strong electric field behaves randomly in a timescale less than the crossover timescale. From the view of fractal dynamics (Sahimi & Arbabi, 1996), such a random behavior in short timescales means that the lightning initiation may involve the heterogeneities of the electric field in the thunderstorm. Initially, small-scale discharge events may occur randomly due to local heterogeneities of the electric field (random phase). Once the electric field increases to certain level in an extensive region in the thunderstorm, these locally occurring small-scale discharge events begin to interact and merge, leading to a great degree of a forthcoming global instability and a catastrophic event, the lightning flash.

There is also a long-standing and fundamental problem about the lightning initiation. Most of lightning initiation mechanisms involve the local electric field intensification, such as the hydrometeor-initiated positive streamer, cosmic ray-initiated runaway breakdown, or beam plasma-like instability (Petersen et al., 2008; Iudin & Davydenko, 2015; Rison et al., 2016). However, these small-scale breakdowns may only serve as an exogenous trigger factor, such as a "lightning seed" (Tran & Rakov, 2016). Only when it is in a highly correlated extensive strong electric field region a lightning seed (a small-scale breakdown) could grow into a large-scale lightning flash, while it could not evolve into a large-scale lightning flash when in a less correlated electric field region. In other words, the establishment of a highly correlated electric field region, hence the occurrence of a lightning flash, is highly subjected to the common electrification process in a thunderstorm.

Acknowledgments
The work leading to this paper was supported by the National Natural Science Foundation of China (grant 41375010) and the Research Grant Council of Hong Kong Government (grant PolyU 152139/15E). LDAR data used in this study are available from the Global Hydrology Resource Center: ftp://ghrc.nsstc.nasa.gov/pub/data/ksc-ldar/.

References

Abe, S., & Suzuki, N. (2012). Universal law for waiting internal time in seismicity and its implication to earthquake network. *Europhysics Letters*, *97*(4), 49002. https://doi.org/10.1209/0295-5075/97/49002

Bak, P., Tang, C., & Wiesenfeld, K. (1987). Self-organized criticality: An explanation of 1/f noise. *Physical Review Letters*, *59*(4), 381–384. https://doi.org/10.1103/PhysRevLett.59.381

Boccippio, D. J., Heckman, S. J., & Goodman, S. J. (2001). A diagnostic analysis of the Kennedy Space Center LDAR network. 1. Data characteristics. *Journal of Geophysical Research*, *106*(D5), 4769–4786. https://doi.org/10.1029/2000JD900687

Bruning, E. C., & Thomas, R. J. (2015). Lightning channel length and flash energy determined from moments of the flash area distribution. *Journal of Geophysical Research: Atmospheres*, *120*, 8925–8940. https://doi.org/10.1002/2015JD023766

Da Silva, C. L. (2015). Numerical modeling of leader discharge mechanisms in lightning, blue jets, gigantic jets, and sprites (PhD thesis). The Pennsylvania State University.

Gou, X., Chen, M., Du, Y., & Dong, W. (2010). Fractal dynamics analysis of the VHF radiation pulses during initial breakdown process of lightning. *Geophysical Research Letters*, *37*, L11808. https://doi.org/10.1029/2010GL043178

Hansen, A. E., Fuelberg, H. E., & Pickering, K. E. (2010). Vertical distributions of lightning sources and flashes over Kennedy Space Center, Florida. *Journal of Geophysical Research*, *115*, D14203. https://doi.org/10.1029/2009JD013143

Hayakawa, M., Nakamura, T., Iudin, D., Michimoto, K., Suzuki, T., Hanada, T., & Shimura, T. (2005). On the fine structure of thunderstorms leading to the generation of sprites and elves: Fractal analysis. *Journal of Geophysical Research*, *110*, D06104. https://doi.org/10.1029/2004JD004545

Hayakawa, M., Iudin, D. I., & Trakhtengerts, V. Y. (2008). Modeling of thundercloud VHF/UHF radiation on the lightning preliminary breakdown stage. *Journal of Atmospheric and Solar - Terrestrial Physics*, *70*(13), 1660.

Huang, Y., Ouillon, G., Saleur, H., & Sornette, D. (1997). Spontaneous generation of discrete scale invariance in growth models. *Physical Review E*, *55*(6), 6433–6447. https://doi.org/10.1103/PhysRevE.55.6433

Iudin, D. I., & Davydenko, S. S. (2015). Fractal model of a compact intra-cloud discharge: I. Features of the structure and evolution. *Radio physics and Quantum Electronics*, *58*(7), 477–496. https://doi.org/10.1007/s11141-015-9621-2

Krehbiel, P. R., Thomas, R. J., Rison, W., Hamlin, T., Harlin, J., & Davis, M. (2000). GPS-based mapping system reveals lightning inside storms. *Eos, Transactions of the American Geophysical Union*, *81*(3), 21–25. https://doi.org/10.1029/00EO00014

Lennon, C., & Maier, L. (1991). Lightning mapping system. In *Proc*. *Int*. *Aerospace and Ground Conf*. *on Lightning and Static Electricity* (pp. 89–1–89-10). Cocoa Beach, FL: NASA.

Maier, L., Lennon, C., Britt, T., & Schaefer, S. (1995). LDAR system performance and analysis. In *The 6th Conf*. *on Aviation Weather Systems*, *Am*. *Meteor*. *Soc*. Boston, Mass.

Mansell, E. R., MacGorman, D. R., Ziegler, C. L., & Straka, J. M. (2002). Simulated three-dimensional branched lightning in a numerical thunderstorm model. *Journal of Geophysical Research*, *107*(D9), 4075. https://doi.org/10.1029/2000JD000244

Mazur, V. (2002). Physical processes during development of lightning flashes. *Comptes Rendus Physique*, *3*(10), 1393–1409. https://doi.org/10.1016/S1631-0705(02)01412-3

Mazur, V. (2016). The physical concept of recoil leader formation. *Journal of Electrostatics*, *82*, 79–87. https://doi.org/10.1016/j.elstat.2016.05.005

McNamara, T. M. (2002). The horizontal extent of cloud-to-ground lightning over the Kennedy Space Center (MSc Thesis) (114 pp.). Air Force Institute of Technology.

Murphy, M. J., Cummins, K. L., & Maier, L. M. (2000). The analysis and interpretation of three dimensional lightning flash information (pp. 102–105). The 16th Int. Conf. on IIPS for Meteorology, Oceanography, and Hydrology.

Nelson, L. A. (2002). Synthesis of 3-dimensional lightning data and radar to determine the distance that naturally occurring lightning travels from thunderstorms (MSc thesis) (85 pp.). OH: Air Force Institute of Technology, Wright-Patterson Air Force Base.

Peng, C. K., Buldyrev, S. V., Havlin, S., Simons, M., Stanley, H. E., & Goldberger, A. L. (1994). Mosaic organization of DNA nucleotides. *Physical Review E*, *49*(2), 1685–1689. https://doi.org/10.1103/PhysRevE.49.1685

Petersen, D., Bailey, M., Beasley, W. H., & Hallett, J. (2008). A brief review of the problem of lightning initiation and a hypothesis of initial lightning leader formation. *Journal of Geophysical Research*, *113*, D17205. https://doi.org/10.1029/2007JD009036

Rakov, V. A., & Uman, M. A. (2003). *Lightning: Physics and effects* (687 pp.). Cambridge University Press.

Riousset, J. A., Pasko, V. P., Krehbiel, P. R., Thomas, R. J., & Rison, W. (2007). Three-dimensional fractal modeling of intra-cloud lightning discharge in a New Mexico thunderstorm and comparison with lightning mapping observations. *Journal of Geophysical Research*, *112*, D15203. https://doi.org/10.1029/2006JD007621

Rison, W., Thomas, R. J., Krehbiel, P. R., Hamlin, T., & Harlin, J. (1999). A GPS-based three-dimensional lightning mapping system: Initial observations in central New Mexico. *Geophysical Research Letters*, *26*(23), 3573–3576. https://doi.org/10.1029/1999GL010856

Rison, W., Krehbiel, P. R., Stock, M. G., Edens, H. E., Shao, X. M., Thomas, R. J., … Zhang, Y. (2016). Observations of narrow bipolar events reveal how lightning is initiated in thunderstorms. *Nature Communications*, *7*, 10721. https://doi.org/10.1038/ncomms10721

Sahimi, M., & Arbabi, S. (1996). Scaling laws for fracture of heterogeneous materials and rock. *Physical Review Letters*, *77*(17), 3689–3692. https://doi.org/10.1103/PhysRevLett.77.3689

Saleur, H., Sammis, C. G., & Sornette, D. (1996). Discrete scale invariance, complex fractal dimensions, and log-periodic fluctuations in seismicity. *Journal of Geophysical Research*, *101*(B8), 17,661–17,677.

Sornette, D. (2004). *Critical phenomena in natural sciences (chaos, fractals, self-organization and disorder: Concepts and tools)*, *Springer Series in Synergetics* (2nd ed.). Heidelberg: Springer.

Stano, G. T., Fuelberg, H. E., & Roeder, W. P. (2010). Developing empirical lightning cessation forecast guidance for the Cape Canaveral Air Force Station and Kennedy Space Center. *Journal of Geophysical Research*, *115*, D09205. https://doi.org/10.1029/2009JD013034

Telesca, L. (2007). Time-clustering of natural hazards. *Natural Hazards*, *40*(3), 593–601. https://doi.org/10.1007/s11069-006-9023-z

Telesca, L., Cuomo, V., Lapenna, V., & Macchiato, M. (2004). Detrended fluctuation analysis of the spatial variability of the temporal distribution of Southern California seismicity. *Chaos, Solitons & Fractals*, *21*(2), 335–342. https://doi.org/10.1016/j.chaos.2003.10.021

Telesca, L., Bernardi, M., & Rovelli, C. (2005). Identifying time-clustering structures in lightning sequences. *Fluctuations and Noise Letters*, *5*(04), 507–514.

Theiler, J., Eubank, S., Longtin, A., Galdrikian, B., & Farmer, J. D. (1992). Testing for nonlinearity in time series: The method of surrogate data. *Physica D*, *58*(1-4), 77–94. https://doi.org/10.1016/0167-2789(92)90102-S

Thomas, R. J., Krehbiel, P. R., Rison, W., Hamlin, T., Harlin, J., & Shown, D. (2001). Observations of VHF source powers radiated by lightning. *Geophysical Research Letters*, *28*(1), 143–146. https://doi.org/10.1029/2000GL011464

Thomas, R. J., Krehbiel, P. R., Rison, W., Hunyady, S. J., Winn, W. P., Hamlin, T., & Harlin, J. (2004). Accuracy of the lightning mapping array. *Journal of Geophysical Research*, *109*, D14207. https://doi.org/10.1029/2004/JD004549

Tran, M. D., & Rakov, V. A. (2016). Initiation and propagation of cloud-to-ground lightning observed with a high-speed video camera. *Scientific Reports*, *6*(1), 39521. https://doi.org/10.1038/srep39521

Turcotte, D. L., Malamud, B. D., Guzzetti, F., & Reichenbach, P. (2002). Self-organization, the cascade model, and natural hazards. *PNAS*, *99*(Supplement 1), 2530–2537. https://doi.org/10.1073/pnas.012582199

Van der Velde, O. A., & Montanya, J. (2013). Asymmetries in bidirectional leader development of lightning flashes. *Journal of Geophysical Research: Atmospheres*, *118*, 13,504–13,519. https://doi.org/10.1002/2013JD020257

Varotsos, P., Sarlis, N. V., Skordas, E. S., Uyeda, S., & Kamogawa, M. (2011). Natural time analysis of critical phenomena. *PNAS*, *108*(28), 11361–11364. https://doi.org/10.1073/pnas.1108138108

Wiens, K. C., Rutledge, S. A., & Tessendorf, S. A. (2005). The 29 June 2000 supercell observed during steps. Part II: Lightning and charge structure. *Journal of the Atmospheric Sciences*, *62*(12), 4151–4177. https://doi.org/10.1175/JAS3615.1

Williams, E. R. (2006). Problems in lightning physics—The role of polarity asymmetry. *Plasma Sources Science and Technology*, *15*(2), S91–S108. https://doi.org/10.1088/0963-0252/15/2/S12

Williams, E. R., & Heckman, S. (2012). Polarity asymmetry in lightning leaders: The evolution of ideas on lightning behavior from strikes to aircraft. *Journal of Aerospace Laboratory*, *5*, 1–8. (AL05–04).

Yair, Y., Aviv, R., Ravid, G., Yaniv, R., Ziv, B., & Price, C. (2006). Evidence for synchronicity of lightning activity in networks of spatially remote thunderstorms. *Journal of Atmospheric and Solar: Terrestrial Physics*, *68*(12), 1401–1415. https://doi.org/10.1016/j.jastp.2006.05.012

Yair, Y. Y., Aviv, R., & Ravid, G. (2009). Clustering and synchronization of lightning flashes in adjacent thunderstorm cells from lightning location networks data. *Journal of Geophysical Research*, *114*, D09210. https://doi.org/10.1029/2008JD010738

Zoghzoghy, F. G., Cohen, M. B., Said, R. K., & Inan, U. S. (2013). Statistical patterns in the location of natural lightning. *Journal of Geophysical Research: Atmospheres*, *118*, 787–796. https://doi.org/10.1002/jgrd.50107